Editors' Choice

ORIGINAL PAPER

Nagoya J. Med. Sci. **87**. 644–663, 2025
doi:10.18999/nagjms.87.4.644

# Acupuncture alleviates the progression of knee osteoarthritis by inhibiting X-inactive specific transcript-mediated activation of the mechanosensitive ion channel Piezo1 signaling

Miaomiao Liu[1,2], Bimeng Zhang[3], Zhaoqin Wang[1,4], Haixin Gou[2,5], Jimeng Zhao[1,4], Maoqing Ye[2,6], Changfeng Song[2,6], Xingang Lu[2], Yan Ji[2], Jie Meng[2], Tao Wu[2,5] and Huangan Wu[1,4]

[1]*Yueyang Hospital of Integrated Traditional Chinese and Western Medicine, Shanghai University of Traditional Chinese Medicine (TCM), Shanghai, China*
[2]*Osteo-Traumatology of Traditional Chinese Medicine, Huadong Hospital, Fudan University, Shanghai, China*
[3]*Department of Acupuncture and Moxibustion, Shanghai General Hospital Shanghai Jiao Tong University School of Medicine, Shanghai, China*
[4]*Shanghai Research Institute of Acupuncture-Moxibustion and Meridian, Shanghai, China*
[5]*Institute of Gerontology, Institute of Integrative Chinese and Western Medicine, Fudan University, Shanghai, China*
[6]*Shanghai Key Laboratory of Clinical Geriatric Medicine, Huadong Hospital, Fudan University, Shanghai, China*

## ABSTRACT

Acupuncture (AP) has been widely used in the treatment of knee osteoarthritis (KOA); however, its underlying molecular mechanisms remain elusive. This study aimed to identify whether acupuncture can relieve KOA progress via inhibiting X-inactive specific transcript (XIST)-mediated Piezo1 activation. The OA cells treated by interleukin (IL)-1β, and rat OA models induced by monosodium iodoacetate were established respectively. The expression of XIST, Piezo1, and extracellular matrix (ECM)-degeneration proteins were evaluated. Cell proliferation was detected by Cell Counting Kit-8 assay. The binding interaction between XIST and Piezo1 was performed using RNA binding protein immunoprecipitation assay (RIP). When XIST is knocked down, apoptosis is significantly reduced, and CHON-001 cell proliferation is increased in comparison to control and IL-1β-induced chondrocytes. Function tests revealed that both in vitro and in vivo, siRNA targeting XIST (si-XIST) increased cell proliferation while preventing apoptosis, ECM degradation, and the production of inflammatory factors. Additionally, we demonstrated that XIST and Piezo1 were bound together via insulin-like growth factor 2 messenger RNA (mRNA) binding proteins 2 (IGF2BP2), with Piezo1 serving as XIST's target. The effects of XIST downregulation were reversed by Piezo1 activation via rescue tests conducted both in vitro and in vivo. Piezo1's expression was reversed after XIST knockdown by IGF2BP2 overexpression. Our findings highlight the therapeutic potential of acupuncture in mitigating the progression of KOA by targeting the XIST-mediated activation of the Piezo1 pathway. By inhibiting this pathway, acupuncture may offer a promising approach to ameliorate the symptoms and slow the progression of KOA.

Keywords: acupuncture, knee osteoarthritis, lncRNA X-inactive specific transcript, mechanosensitive ion channel, Piezo1 protein

Received: December 9, 2024; accepted: February 20, 2025

Corresponding Author: Huangan Wu, MD
Shanghai Research Institute of Acupuncture-Moxibustion and Meridian, No. 650 South Wanping Road, Xuhui District, Shanghai 200030, China
Tel: +86-021-65161782, Fax: +86-021-62498628, E-mail: WUHuangan000@163.com

Abbreviations:
ADAMTS: a disintegrin and metalloproteinase with thrombospondin
AP: acupuncture
cDNA: complementary DNA
CG: control group
COL2A1: collagen type II alpha 1
ECM: extracellular matrix
ELISA: enzyme-linked immunosorbent assay
IGF2BP2: insulin-like growth factor 2 mRNA binding proteins 2
IL: interleukin
KOA: knee osteoarthritis
lncRNA: long non-coding RNA
MG: model group
MMP: matrix Metalloproteinase
mRNA: messenger RNA
siRNA: small interfering RNA
SOX9: sex determining region Y box protein 9
TNF: tumor necrosis factor
XIST: X-inactive specific transcript

This is an Open Access article distributed under the Creative Commons Attribution-NonCommercial-NoDerivatives 4.0 International License. To view the details of this license, please visit (http://creativecommons.org/licenses/by-nc-nd/4.0/).

## INTRODUCTION

Knee osteoarthritis (KOA), also known as osteoarthritis of the knee, degenerative joint disease of the knee, or knee joint degenerative osteoarthritis, is a degenerative disease of the knee joint. Clinically, it is often characterized by knee joint pain, stiffness, crepitus, limited mobility, joint deformity, difficulty walking, and other symptoms. This illness mostly affects middle-aged and older people in China, and it is more common in females than in males.[1] KOA can lead to a decline in patients' quality of life and psychological changes. The occurrence of KOA is strongly associated with factors like knee joint trauma, low bone density, muscle weakness, joint laxity, advanced age, female gender, obesity, and frequent squatting.[2] During the OA development process, the duration and severity of the disease change with the production and interaction of inflammatory factors.[3] Inflammatory factors are the main cause of pain symptoms in KOA patients, and many inflammatory factors can be detected in patients' physiological indicators. Inflammatory factors participate in the metabolism of KOA and play a vital role in preserving the stability of the joint environment. Clinical treatment of KOA mainly focuses on symptomatic treatment, including hyaluronic acid, intra-articular injections of steroids, opioid medications, oral non-steroidal anti-inflammatory drugs and other drugs.[4] However, these treatments are associated with various adverse reactions such as gastrointestinal ulcers, thromboembolism, prosthetic loosening, and nerve damage. Joint replacement surgery is also one of the methods for treating KOA, but surgical treatment may lead to complications and long recovery periods, especially in patients with poor tolerance, particularly older adults with multiple underlying diseases.[5] Traditional Chinese medicine external treatment and rehabilitation methods have the advantages of being non-invasive, simple, convenient, safe, and effective, and are easily accepted by patients.[6,7] It has been reported that acupuncture (AP), moxibustion, and needle-knife therapy are beneficial for patients with KOA. In the last several years, AP therapy has been extensively used in the clinical treatment of KOA due to its safety, reliability, and definite therapeutic effects.[8]

Piezo1 protein (mechanosensitive ion channel protein 1) is a novel ion channel protein closely associated with mechanical stress signaling.[9] Piezo1 protein can respond to various forms of

mechanical stimuli, such as stretching, fluid shear force, hydrostatic pressure, etc, and selectively permeate multiple ions,[10] primarily calcium ($Ca^{2+}$). The sensitivity of Piezo1 to mechanical stress is intrinsic and does not require any other cellular components. Additionally, Piezo1 protein has been shown to be expressed in human cartilage and may participate in the process of chondrocyte death,[11] even if it's still unclear exactly how it works.

Long non-coding RNAs (lncRNAs) are a significant category of genetic regulatory factors in the human genome, directly regulating processes such as transcription factor activity and protein translation, thereby influencing diseases.[12] X-inactive specific transcript (XIST), as a type of lncRNA, is prominently shown in cartilage tissues of arthritis and interleukin (IL)-1β-treated cartilage tissues.[13] Knocking down XIST can inhibit the progression of arthritis, laying a good foundation for targeted therapy for arthritis.[14] There is conjecture that XIST could have a comparable function in elderly KOA. Recent studies have found elevated levels of XIST in the serum of elderly KOA patients,[14,15] and its relationship with disease severity and inflammatory factor levels is closely related, which may have certain significance for guiding clinical treatment of KOA patients. Currently, there is extensive research on XIST in cancer, where it can regulate diseases by modulating processes like cancer cell invasion, proliferation and metastasis.[16] Here, our study's objective is to look at the potential therapeutic effect of AP in alleviating the progression of KOA. Specifically, the study aims to explain the mechanism by which AP prevents the activation of the mechanosensitive ion channel Piezo1 signaling, mediated by the lncRNA XIST. The goal is to provide insights into the molecular pathways underneath the beneficial consequences of AP on KOA and to explore XIST as a possible therapy objective for managing this condition.

## METHODS

*The OA cell model was established*

The CHON-001 cell line from the Shanghai Cell Bank of Chinese Academy of Sciences (Shanghai, China) exposed to IL-1β represents a suitable in vitro model for studying OA.[17] As a result, this research chose to use this paradigm. The Roswell Park Memorial Institute (RPMI)-1640 media (Gibco, US) supplemented with 10% fetal bovine serum (FBS) (Gibco, US) and 2 mM glutamine (Gibco, US) was used to cultivate the human chondrocyte cell line CHON-001 at 37 °C and 5% carbon dioxide ($CO_2$). Then, during a 48-hour incubation period at room temperature, IL-1β was applied to the CHON-001 cells at a concentration of 10 ng/mL.

*Animals and establishment of OA model*

The OA model was built by intra-articular injection of monosodium iodoacetate (Sigma-Aldrich, St. Louis, MO, US) based on the previous study.[18,19] The animals were kept in cages with three to a room, each with a regulated temperature of 21 to 22 degrees Celsius, access to sterile food and drink, as well as a 12-hour cycle of light and dark. Each group used three animals, and each group conducted six separate tests to determine the in vivo effectiveness. Rats were shaved of the hair above their right knee joints and given anaesthesia using isoflurane (1–2.5% maintenance, 1–3% induction). Using a 26.5-gauge needle, a sterile 0.9% normal saline solution containing 5 μL of monosodium iodoacetate (5 mg/mL) was introduced into the right knee joint via the sub-patellar ligament. The Animal Research Ethics Committee of Yueyang Hospital of Integrated Traditional Chinese and Western Medicine, Shanghai University of Traditional Chinese Medicine reviewed and approved all experimental protocols to ensure they complied with the guidelines set out by the China Council for Animal Care and Use. Before the trial started, the animals were divided into treatment groups at random. An equal amount of phosphate buffered

solution (PBS) was delivered into control animals by injection.

*Sample collection*

Injections were administered to the right knee joint 28 days later. Rats were placed in a supine position after pentobarbital sodium anesthesia (isoflurane, 1–1.5% maintenance, 2–3% induction), with the chest cavity exposed. A total of 50 milliliters of saline was injected into the rats via the heart until the lungs, liver, and limbs turned white. Subsequently, 30 milliliters of 4% paraformaldehyde were injected, leading to tail and limb tremors. The right knee joint was fixed for 24 hours in 4% paraformaldehyde and then decalcified for 20 days in a 10% ethylene diamine tetraacetic acid (EDTA) (pH=7.4) solution. After tissue dehydration, paraffin embedding was performed, and continuous sections of 4 micrometers thick were prepared.

*Detection of tumor necrosis factor-α and IL-6 utilizing enzyme-linked immunosorbent assay*

Samples from study animals or experimental cells were collected using appropriate protocols. Reconstitute the lyophilized standards provided in the Enzyme-Linked Immunosorbent Assay (ELISA) kit (Thermo Fisher Scientific) with the appropriate volume of assay diluent to obtain a series of standard solutions with known concentrations of tumor necrosis factor (TNF)-α and IL-6. The serum samples were diluted utilizing an appropriate sample diluent provided in the ELISA kit. Typically, a 1:2 or 1:5 dilution of serum with sample diluent is recommended. Adjust dilution factors based on the expected concentration of TNF-α and IL-6 in the serum. The ELISA plate wells were labelled according to the protocol. The specified wells were filled with the prepared standard solutions and diluted samples. The ELISA plate was raised at room temperature or at a specified temperature for a defined period according to the manufacturer's instructions. Wash the plate wells multiple times (3–4 times) with wash buffer to eliminate unbound materials. TNF-α and IL-6 detection antibodies were included into the wells. Each well was filled with substrate solution, and the plate was then raised in the dark until colour developed. The addition of a stop solution terminated the colour development response. A microplate reader accustomed to calculating the absorbance at a specific wavelength (typically 450 nm with a reference wavelength) for each well.

*Reverse transcriptase-quantitative polymerase chain reaction*

After the cells of interest have had their total RNA isolated, put the samples on ice to dissolve them. Quantify 1000 ng of RNA per sample according to the iScript cDNA Synthesis Kit (BIO-RAD, Hercules, California, US) instructions (if the sample concentration exceeds 1000 ng/μL, dilute to 500 ng/μL).

After synthesizing complementary DNA (cDNA), store it at –20 °C for future use. Retrieve the synthesized cDNA template and keep it on ice. Dilute the cDNA template with an equal volume of double-distilled water ($ddH_2O$). Subsequently, according to the iTaq Universal SYBR Green Supermix kit instructions (Bio-Rad, US), add the solutions to each well of a 96-well polymerase chain reaction (PCR) reaction plate. Top up to 10 μL with $ddH_2O$. Prepare 3 technical replicates for each reaction well. After sample addition, apply adhesive film around the edges of the 96-well plate to ensure a tight seal. Before beginning the reaction, centrifuge at 3500 rpm and 4 °C for 5 minutes to get rid of any air bubbles. Use glyceraldehyde-3-phosphate dehydrogenase (GAPDH) as the internal reference gene. The primer sequences are shown in Table 1.

**Table 1** Primer sequence

| Genes | Forward (5′-3′) | Reverse (5′-3′) |
|---|---|---|
| SOX9 (Rats) | AGCTGATCGCGACAGTCTCT | GCTGACGGGTGAGAGGTTTC |
| SOX9 (Human) | AGGAAGCTCGCGGACCAGTAC | GGTGGTCCTTCTTGTGCTGCAC |
| COL2A1 (Rats) | AGTGGAGGAGGAGATGAGG | TGGGAAGTAGAGCGGTAGG |
| COL2A1 (Human) | CCTGGCAAAGATGGTGAGACAG | CCTGGTTTTCCACCTTCACCTG |
| Aggrecan (Rats) | TGGCTGACTTCAGGTGAGGA | CCTGGTCCCTTTGACCTCTG |
| Aggrecan (Human) | CTAGTGGACTCCCTTCAGGAAC | CGCTAAGCTCAGTCACTCCAG |
| ADAMTS-4 (Rats) | AGCTGGTGCTGAGGTGATGT | CCATGTCGAGGCTCAGATGA |
| ADAMTS-4 (Human) | TCACTGACTTCCTGGACAATGGC | GGTCAGCATCATAGTCCTTGCC |
| MMP3 (Rats) | AGGCTGGTGGCAGACTATGG | GCCAGGCTCTGATGCTCTTG |
| MMP3 (Human) | CACTCACAGACCTGACTCGGTT | AAGCAGGATCACAGTTGGCTGG |
| MMP13 (Rats) | GAGCGAGAAGACGGCAGTTC | CAGGAAATCACAGCACAGCA |
| MMP13 (Human) | CCTTGATGCCATTACCAGTCTCC | AAACAGCTCCGCATCAACCTGC |
| XIST (Rats) | AAGTCTTCAAAACACCCAAG | CTTCCCACCAACTGTGAAAA |
| XIST (Human) | GTAGGTGTGCTGATAACCAAGGC | GGGAAAGGAAGATTGAGGGTGG |
| Piezo1 (Rats) | FTACTGGCTGTTGCTACCCTG | CCTGTGTGACCTGGTATGCT |
| Piezo1 (Human) | CCTGGAGAAGACTGACGGCTAC | ATGCTCCTTGGATGGTGAGTCC |
| GAPDH (Rats) | GAAGGTGAAGGTCGGAGTC | GAAGATGGTGATGGGATTTC |
| GAPDH (Human) | GTCTCCTCTGACTTCAACAGCG | ACCACCCTGTTGCTGTAGCCAA |

*Western blotting assay*

To extract proteins from tissues and cells, Beyotime Biotechnology in China's radio immunoprecipitation assay (RIPA) lysis buffer was used. Bradford Protein Assay Kit (Beyotime Biotechnology, China) was used to measure the proteins' concentration and purity. Using a 10% sodium dodecyl sulfate-polyacrylamide gel (SDS-PAGE), the proteins were separated before being transferred to polyvinylidene fluoride (PVDF) membranes. Subsequently, the membranes were incubated at 4 °C for the whole night with primary antibodies. The membranes were then exposed to room temperature for one hour before being inoculated with the secondary antibody, goat anti-rabbit immunoglobulin G (IgG) (1:2000, PR30011, Proteintech). An enhanced chemiluminescence system from Millipore was used to see the protein bands, and Image Lab software from BioRad, US was used to analyze the band intensities. OriGene Wuxi Biotechnology (Wuxi, China) provided the primary antibodies, which were anti- sex determining region Y box protein 9 (SOX9) (1:500, AP06583PU-N), anti-aggrecan (1:1000, TA336492), anti-collagen type II alpha 1(COL2A1) (1:1000, R1039X), anti-a disintegrin and metalloproteinase with Thrombospondin 4 (ADAMTS-4) (1:2000, TA805208), anti-matrix metalloproteinase (MMP) 3 (1:500, AP06233PU-N), and anti-MMP13 (1:4000, TA506806).

*Cell counting Kit-8 assay*

Cell viability was established through Cell Counting Kit-8 assay after the manufacturer's guidelines (Protentech, Wuhan, China). Chondrocytes were plated in 96-well plates, with $1 \times 10^4$ cells per well. Post incubation, each well received 10 μL of Cell Counting Kit-8 solution and was left to incubate for 2 hours. A spectrophotometric microplate reader accustomed to assess the absorbance at 450 nm.

*Subcellular fractionation assay*

The nuclear and cytoplasmic components were separated using the PARISTM Kit (Invitrogen, US) based on the manufacturer's instructions. To summarize, 600 μL of resuspension buffer was used to suspend CHON-001 cells ($5 \times 10^6$ cells) for a duration of 15 minutes. Then, following centrifugation at 400 × g for 15 minutes, the cytoplasmic fraction was extracted from the supernatant. After that, the pellet was reconstituted for 20 minutes in 300 μL of PBS, nuclear isolation buffer, and RNase-free water. Nuclear fractionation was applied to the pellet after centrifugation. Using reverse transcriptase-quantitative PCR (RT-qPCR), the expression levels of the lncRNAs, XIST, GAPDH, and U6 were measured.

*RNA binding protein immunoprecipitation assay*

Cells were lysed using a suitable lysis buffer to release cellular contents while preserving protein-protein interactions. Antibodies against insulin-like growth factor 2 messenger RNA (mRNA) binding proteins 2 (IGF2BP2) (Proteintech, cat no. 11601-1-AP) were coupled to protein A/G magnetic beads to capture IGF2BP2-bound complexes. The antibody-bound magnetic beads were then treated with the cell lysate, allowing for the formation of complexes between IGF2BP2 and its interacting partners, including Piezo1. The beads were washed extensively to remove non-specifically bound proteins and contaminants, ensuring the specificity of the interactions captured. Bound complexes were eluted from the beads, releasing the proteins associated with IGF2BP2, including any Piezo1 molecule that were enriched. The data obtained from the protein immunoprecipitation (RIP) assay were analyzed to assess the degree of enrichment of Piezo1 to IGF2BP2, providing insights into their potential interaction and functional relevance.

*Experiment for mRNA stability*

Suitable cell lines expressing Piezo1 mRNA were cultured under standard conditions, maintaining proper growth and viability. Transcription was halted by addressing the cells with a transcription inhibitor such as actinomycin D or 5,6-dichloro-1-beta-D-ribofuranosylbenzimidazole (DRB), which prevents the synthesis of new mRNA molecules. Total RNA was taken from the harvested cells utilising a suitable RNA extraction kit, ensuring the preservation of RNA integrity. Spectrophotometry and fluorometry were used to measure the isolated RNA's content and purity. Reverse transcriptase enzyme and oligo(dT) primers were used to reverse transcribe extracted RNA into cDNA in order to collect mRNA molecules. The RT-qPCR was performed to quantify the abundance of Piezo1 mRNA at each time point. Specific primers targeting Piezo1 mRNA were used for amplification, and a housekeeping gene (GAPDH) served as an internal control for normalization.

*Statistical analysis*

Software called GraphPad Prism 9.0 (GraphPad Software) was employed in this study's statistical analysis. The mean ± standard deviation (SD) of the triple experiment results were shown. One-way or two-way analysis of variance, as well as the Student's t-test, were employed for group comparisons. A significance level of less than 0.05 was used for the p-value.

## RESULTS

*Successful establishment of OA cell model in vitro*

IL-1β adds to the degradation of articular cartilage; consequently, 10 ng/mL IL-1β was administered for 24 hours on CHON-001 cells to establish an in vitro model of OA. In contrast

to the control group (CG), aggrecan expression was considerably downregulated in IL-1β-treated CHON-001 cells (Fig. 1A), while the expression level of MMP13 increased (Fig. 1B). The decrease in aggrecan and the increase in MMP13 expression indicate the accomplishment of creating the in vitro OA cell model.

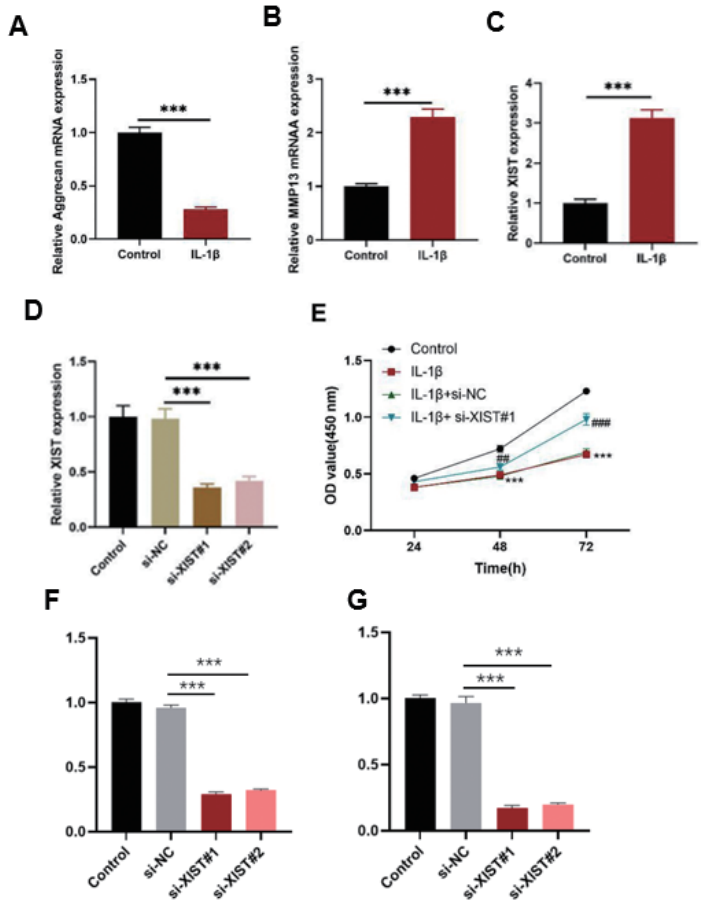


**Fig. 1** XIST knockdown inhibits apoptosis and proliferation of CHON-001 cells
(A) *Aggrecan*, (B) *MMP13* and (C) lncRNA *XIST* mRNA levels. (D) Transfection efficiency, (E) cell proliferation. In relation to IL-1β+si-NC, *$P < 0.05$, **$P < 0.01$, ***$P < 0.001$; ##$P < 0.01$, ###$P < 0.001$ exist.
XIST: X-inactive specific transcript
MMP: matrix metalloproteinase
IL: interleukin
NC: normal control
mRNA: messenger RNA
lncRNA: long non-coding RNA
si-XIST: siRNA targeting XIST
si-NC: siRNA negative control
OD: optical density

*Knockdown of XIST markedly promotes the proliferation of CHON-001 cells*

RT-qPCR was carried out to find the expression level of XIST in CHON-001 cells to confirm the change of XIST mRNA post-treatment of IL-1β and transfection efficiency. After IL-1β stimulation, lncRNA XIST level was increased remarkably compared with control cells (Fig. 1C). Compared to the CG, XIST small interfering RNA 1 (siRNA1) considerably reduced the expression level of XIST in CHON-001 cells (Fig. 1D). However, the impact of XIST siRNA2 on XIST expression was limited compared to the CG (Fig. 1D); consequently, XIST siRNA1 was selected for further investigations.

To further validate the specificity of XIST knockdown, we conducted parallel experiments using both siRNA1 and siRNA2. As shown in Fig. 1F, both siRNA1 and siRNA2 significantly reduced XIST expression compared to the CG ($p < 0.01$). The knockdown efficiency of siRNA1 (82.3 ± 4.2%) was comparable to that of siRNA2 (79.8 ± 3.9%), with no statistically significant difference between them ($p > 0.05$). Furthermore, both siRNAs showed similar effects on downstream targets, including Piezo1 expression (Fig. 1G). These results confirm that the observed effects are specifically due to XIST knockdown rather than off-target effects.

5-ethynyl-2′-deoxyuridine (EdU) staining in conjunction with the Cell Counting Kit-8 test accustomed to measure cell proliferation. Cell vitality was much lower after IL-1β treatment in contrast to the CG, but siRNA targeting XIST (si-XIST) dramatically enhanced cell viability. Moreover, in contrast to the IL-1β group, si-XIST restored the cell viability of IL-1β-induced chondrocytes (Fig. 1E). These findings suggest that XIST knockdown increases CHON-001 cell growth.

*Effect of lncRNA XIST on extracellular matrix gene and inflammatory factor levels in in-vitro model of OA*

In this study, we investigated the function of XIST in the progression of OA in vitro through functional experiments. We also looked at the mRNA expression of genes linked to extracellular matrix (ECM) (Aggrecan, COL2A1 and SOX9) and genes related to ECM breakdown (MMP13, MMP3 and ADAMTS-4). As seen in Fig. 2A-F, in contrast to the CG, the expression of SOX9, COL2A1, and Aggrecan considerably decreased in IL-1β-induced chondrocytes, while ADAMTS-4, MMP3, and MMP13 increased. However, the previous phenotype was restored by si-XIST in contrast to the IL-1β group. Additionally, in IL-1β-treated CHON-001 cells, the levels of TNF-α and IL-6 significantly increased, but this effect was notably attenuated after XIST knockdown (Fig. 2G). Our findings suggest that XIST functioned as a promoter in OA and that knockdown of XIST can attenuate the promoting effect of XIST on OA.

*Overexpression of Piezo1 in OA model cells can reverse the effect of lncRNA XIST knockdown*

First, IL-1β-treated CHON-001 cells were transfected, and PCR accustomed to detecting the transfection efficiency of Piezo1 overexpression in the cell line (Fig. 3A). Subsequently, the ECM-related genes *Aggrecan*, *COL2A1* and *SOX9*, as well as the ECM degradation genes *MMP13*, *MMP3* and *ADAMTS-4*, were evaluated for changes in gene expression in each group using PCR analysis. Our findings revealed that si-XIST#1 considerably increased the mRNA levels of *COL2A1*, *Aggrecan* and *SOX9*, while decreasing the protein levels of *MMP3*, *MMP13* and *ADAMTS-4*. However, these effects induced by si-XIST#1 were reversed when Piezo1 was overexpressed (Fig. 3B). Additionally, XIST knockdown could reverse the effects of IL-1β on CHON-001 cells; however, Piezo1 overexpression could reverse the impacts of si-XIST#1.

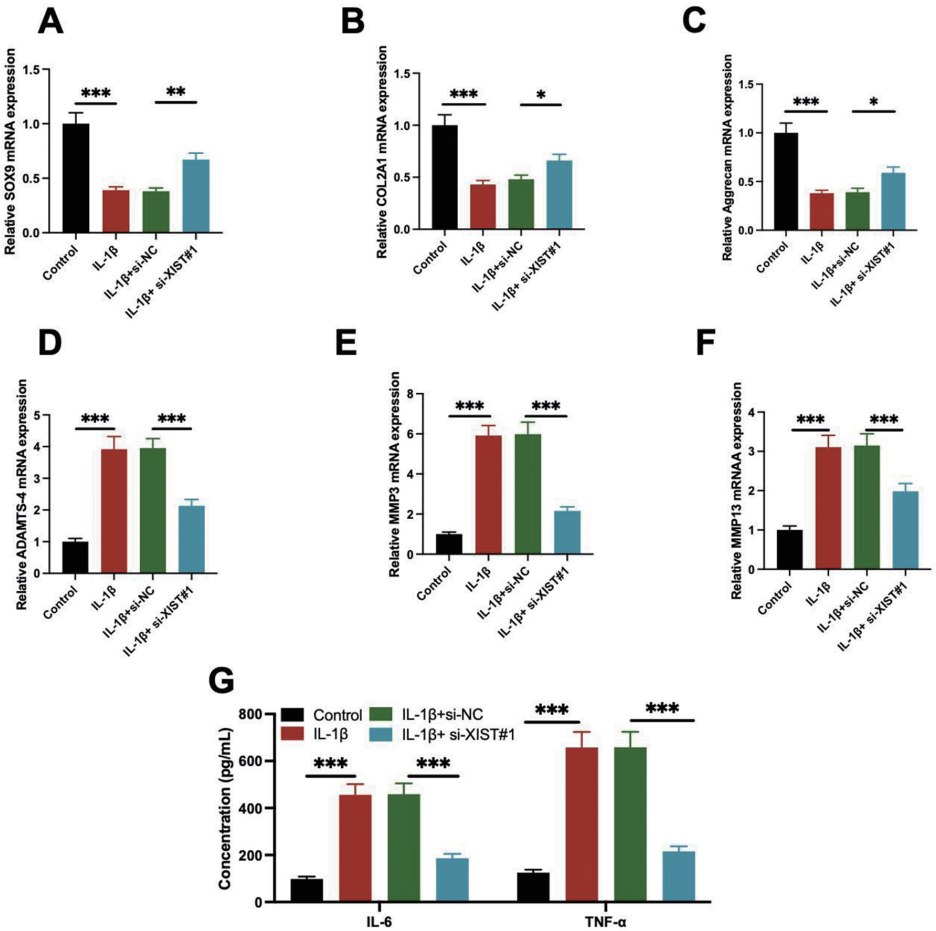


**Fig. 2** Downregulation of XIST inhibits ECM-degeneration and levels of inflammatory factors in IL-1β-induced chondrocytes

(A)–(F) After IL-1β stimulation and lncRNA XIST knockdown, the mRNA levels of MMP13, MMP3, ADAMTS-4, Aggrecan, COL2A1 and SOX9; (G) IL-6 and TNF-α levels was tested during IL-1β treatment and knockdown of lncRNA XIST. $^{*}P < 0.05$, $^{**}P < 0.01$, $^{***}P < 0.001$.

IL: interleukin
XIST: X-inactive specific transcript
ECM: extracellular matrix
MMP: matrix metalloproteinase
ADAMTS: a disintegrin and metalloproteinase with thrombospondin
COL2A1: collagen type II alpha 1
SOX9: sex determining region Y box protein 9
TNF: tumor necrosis factor
mRNA: messenger RNA
lncRNA: long non-coding RNA
si-XIST: siRNA targeting XIST
si-NC: siRNA negative control

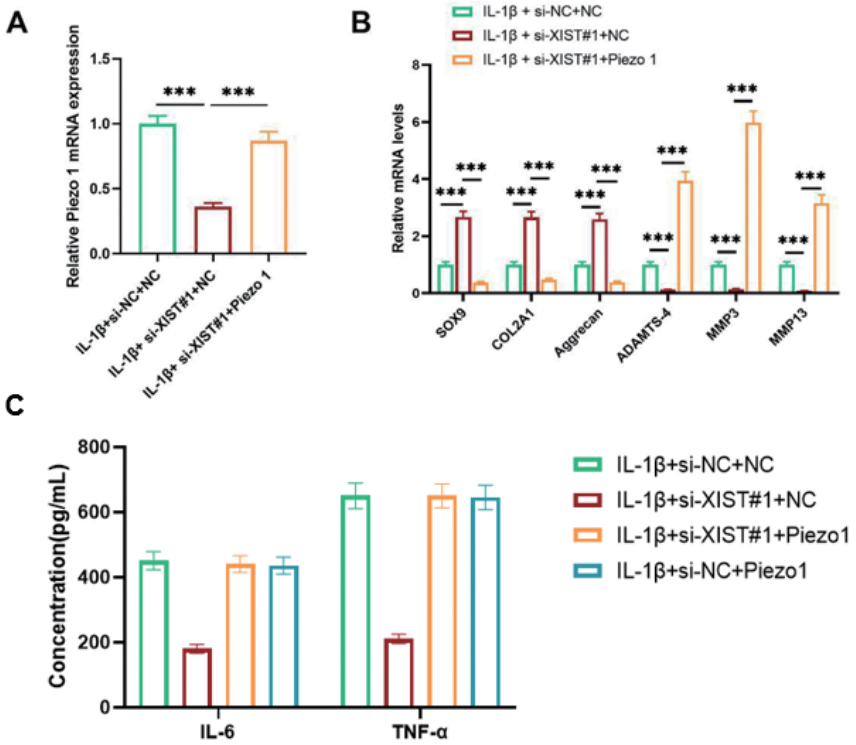


**Fig. 3** Overexpression of Piezo1 reverses effects of XIST silencing on IL-1β-induced chondrocytes
(A) Effectiveness of Piezo1 overexpression. After IL-1β stimulation, IL-1β stimulation + si-XIST, and IL-1β stimulation + si-XIST + Piezo1 expression, (B) the mRNA levels of Aggrecan, MMP13, MMP3, ADAMTS-4, COL2A1 and SOX9. (C) TNF-α and IL-6 levels was tested utilizing ELISA assay. $^{*}P < 0.05$, $^{**}P < 0.01$, $^{***}P < 0.001$.
XIST: X-inactive specific transcript
IL: interleukin
ADAMTS: a disintegrin and metalloproteinase with thrombospondin
MMP: matrix metalloproteinase
COL2A1: collagen type II alpha 1
SOX9: recombinant sex determining region Y box protein 9
TNF: tumor necrosis factor
mRNA: messenger RNA
si-XIST: siRNA targeting XIST
si-NC: siRNA negative control
ELISA: enzyme-linked immunosorbent assay

To establish the specificity of the XIST-Piezo1 pathway, we included an additional CG combining IL-1β treatment with siRNA negative control (si-NC) and Piezo1 overexpression. As demonstrated in Fig. 3C, Piezo1 overexpression in the presence of IL-1β and si-NC resulted in significant changes in ECM-related genes, with decreased expression of SOX9, COL2A1, and Aggrecan, and increased expression of MMP13, MMP3, and ADAMTS-4 ($p < 0.01$). These changes were comparable to those observed in the IL-1β + si-XIST + Piezo1 overexpression group, confirming that Piezo1 activation can promote OA progression independently of XIST expression levels.

*LncRNA XIST promotes Piezo1 expression through IGF2BP2 pathway*

Our investigation into the regulatory mechanism between lncRNA XIST and Piezo1 was conducted using the lncATLAS website (http://lncatlas.crg.eu). The subcellular fractionation test (Fig. 4B) supported our findings that lncRNA XIST was mostly found in the nucleus (Fig. 4A), indicating that it could have a role in transcriptional control. To investigate the regulation of Piezo1 by XIST expression, we conducted PCR experiments to observe changes in Piezo1 expression when XIST was knocked down and IGF2BP2 was overexpressed. The results showed that si-XIST significantly decreased Piezo1 expression, while IGF2BP2 overexpression reversed this effect (Fig. 4C). In addition, our RIP assay showed the interaction between lncRNA XIST and Piezol protein, finding that Piezo1 was enriched on the IGF2BP2 protein, and si-XIST inhibited this phenomenon (Fig. 4D). Finally, we investigated the result of lncRNA XIST on *Piezo1* mRNA stability and found that si-XIST led to a decrease in *Piezo1* mRNA stability, which was reversed by IGF2BP2 (Fig. 4E).

*AP can effectively relieve the pain behavior of KOA rats*

After inhalation anesthesia using an ABM anesthesia machine, rats were selected based on the Experimental Acupuncture Association's "Atlas of Acupoints for Experimental Animals" and needled at the "Nei Xiyan" (internal knee eye) and "Wai Xiyan" (external knee eye) points located within the depressions at the inner and outer edges of the patellar ligament, respectively. With the rats' knee joints flexed, Huatuo brand needles (0.3 mm × 13 mm) were inserted straight to a depth of 5–8 mm and retained. Electrical stimulation was then applied at a frequency of 2–3 Hz with a sparse-dense wave pattern and an intensity of 1–3 mA, ideally resulting in visible muscle twitching and tremors in the lower limbs. Treatment was administered once per day for 20 minutes per session (Fig. 5A). The sham AP group received needling around the "Nei Xiyan" and "Wai Xiyan" points at superficial depths without connecting to an electrical stimulation device. Treatment was administered once per day for 20 minutes per session. This treatment regimen was conducted for a total of 4 weeks (Fig. 5B).

In the OA rats induced by monosodium iodoacetate (5 μL, 5 mg/mL) combined with sterile 0.9% normal saline, secondary tactile allodynia was measured to evaluate the role of Piezo1 in OA treatment. Paw withdrawal latency experiments indicated a decline in paw withdrawal latency in the model group (MG) in contrast to the CG, paw withdrawal latency increased in the AP group in contrast to the MG, and paw withdrawal latency decreased in the Piezo1 group in contrast to the AP group (Fig. 5C). The plantar mechanical pain threshold experiment showed an expected decrease in paw withdrawal time in the MG in contrast to the CG, PWT increased in the AP group in contrast to the MG, and PWT decreased in the Piezo1 group in contrast to the AP group (Fig. 5D). Additionally, the weight-bearing difference experiment confirmed a decrease in weight-bearing difference in the MG in contrast to the CG, an increase in weight-bearing difference was noted in the AP group in contrast to the MG; weight-bearing difference decreased in the Piezo1 group in contrast to the AP group (Fig. 5E).

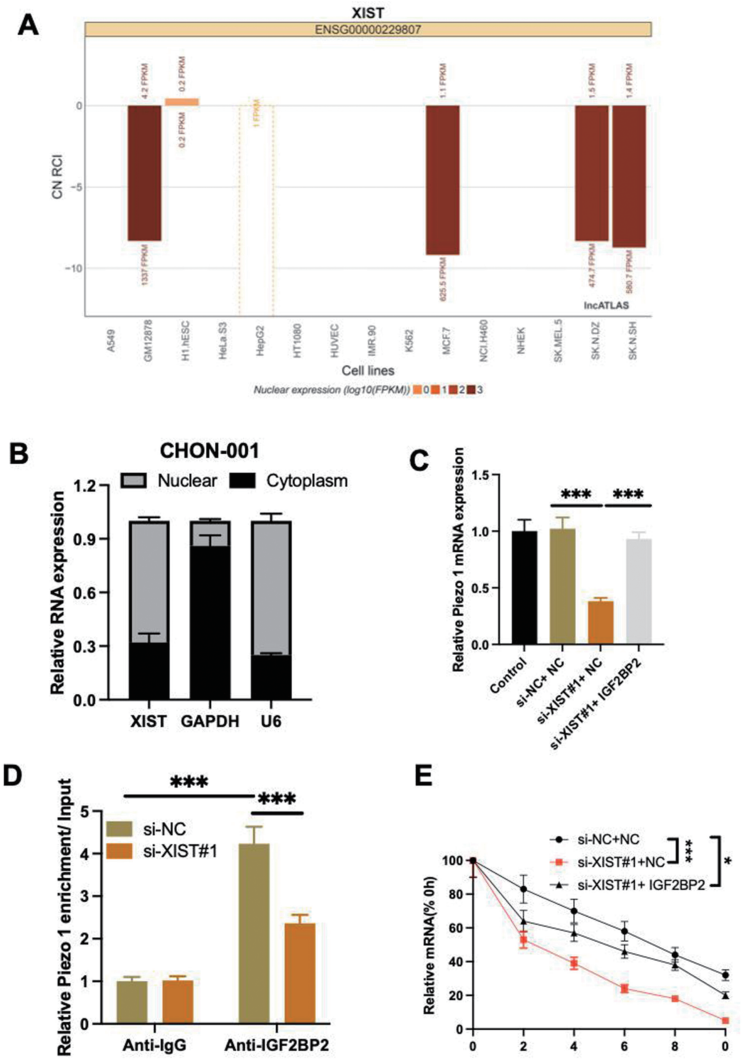


**Fig. 4** LncRNA XIST promotes Piezo1 expression through IGF2BP2 pathway

(A–B) Prediction and determination of subcellular localization of lncRNA XIST using online database and subcellular fractionation test respectively; (C) si-XIST significantly reduced the Piezo1 mRNA, and overexpression of IGF2BP2 reversed this effect; (D) the interplay between lncRNA XIST and Piezo1 was examined by RIP assay; (E) stability of Piezo1 mRNA was decreased and IGF2BP2 overexpression reverses it. $^{*}P < 0.05$, $^{***}P < 0.001$.

XIST: X-inactive specific transcript

IGF2BP2: insulin-like growth factor 2 mRNA binding proteins 2

RIP: binding protein immunoprecipitation assay

mRNA: messenger RNA

lncRNA: long non-coding RNA

si-XIST: siRNA targeting XIST

si-NC: siRNA negative control

GAPDH: glyceraldehyde-3-phosphate dehydrogenase

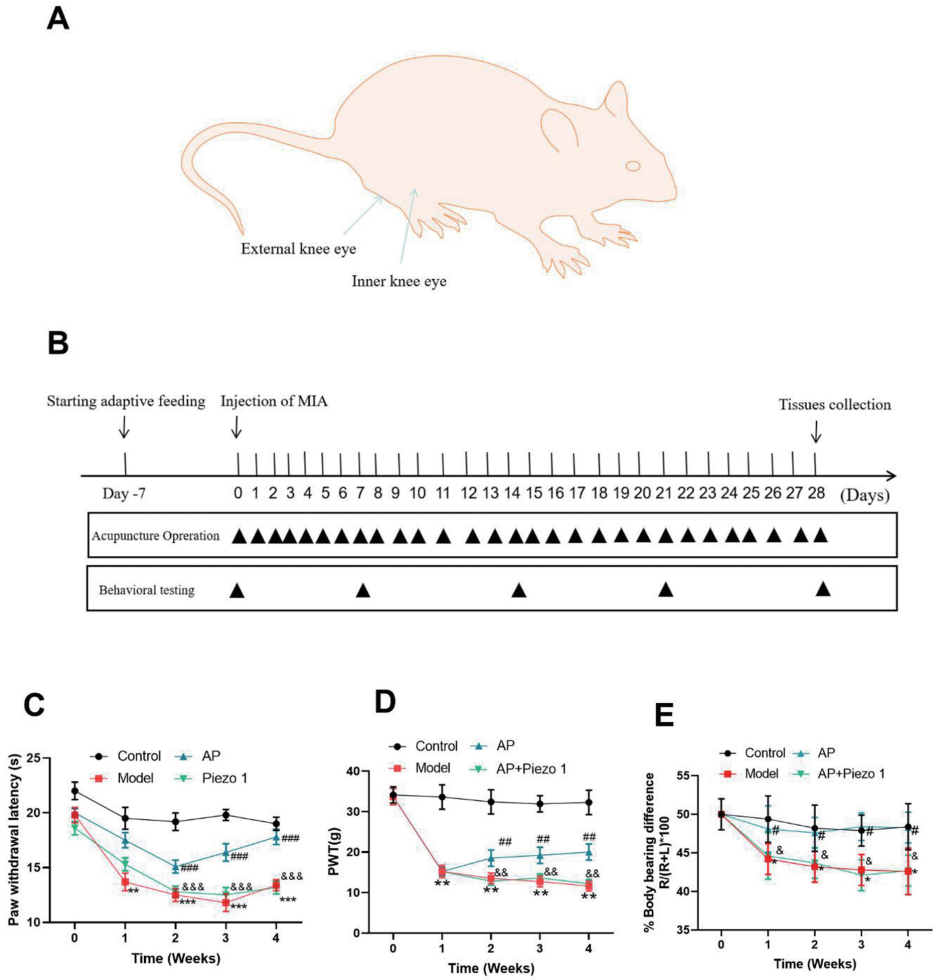


**Fig. 5** AP reduced the pain reactions in KOA rats

(A, B) Scheme of the experimental design. After one-week adaptive feeding, injection of MIA into the knee eye was performed. Rats have been received AP treatment each day for 28 days, behavioral testing was carried out on days 0, 7, 14, 21 and 28. Tissue collection was occurred on the 28th day after the injection of MIA. (C–E) AP treatment can increase in PWL, PWT and body-bearing test compared to OA model group, and activation of Piezo1 can reverse these effects during AP treatment. $^{\&}P < 0.05$, $^{\&\&}P < 0.01$, $^{\&\&\&}P < 0.001$ vs AP; $^{\#}P < 0.05$, $^{\#\#}P < 0.01$, $^{\#\#\#}P < 0.001$ vs model; $^{*}P < 0.05$, $^{**}P < 0.01$, $^{***}P < 0.001$ vs control.

AP: acupuncture
KOA: knee osteoarthritis
MIA: monosodium iodoacetate
PWL: paw withdrawal latency
PWT: paw withdrawal time

*Activation of Piezo1 enhances OA progression in vivo*

Next, we looked at the function of Piezo1 in the progression of OA through functional experiments. We also evaluated the protein and mRNA expression of ECM-related genes (Aggrecan, COL2A1 and SOX9) and ECM degradation genes (MMP13, MMP3 and ADAMTS-4). As seen in Fig. 7A, B, in chondrocytes from the OA model, SOX9, COL2A1, and Aggrecan were significantly decreased, while MMP13, MMP3 and ADAMTS-4 were increased. In animals treated with AP, chondrocytes showed decreased levels of Aggrecan, COL2A1 and SOX9, and increased levels of ADAMTS-4, MMP3, and MMP13. However, in animals stimulated with Piezo1 agonist after AP treatment, the levels of Aggrecan, COL2A1 and SOX9 decreased significantly again, while the levels of MMP13, MMP3 and ADAMTS-4 increased significantly, showing no significant difference in contrast to the OA MG (Fig. 6A, B).

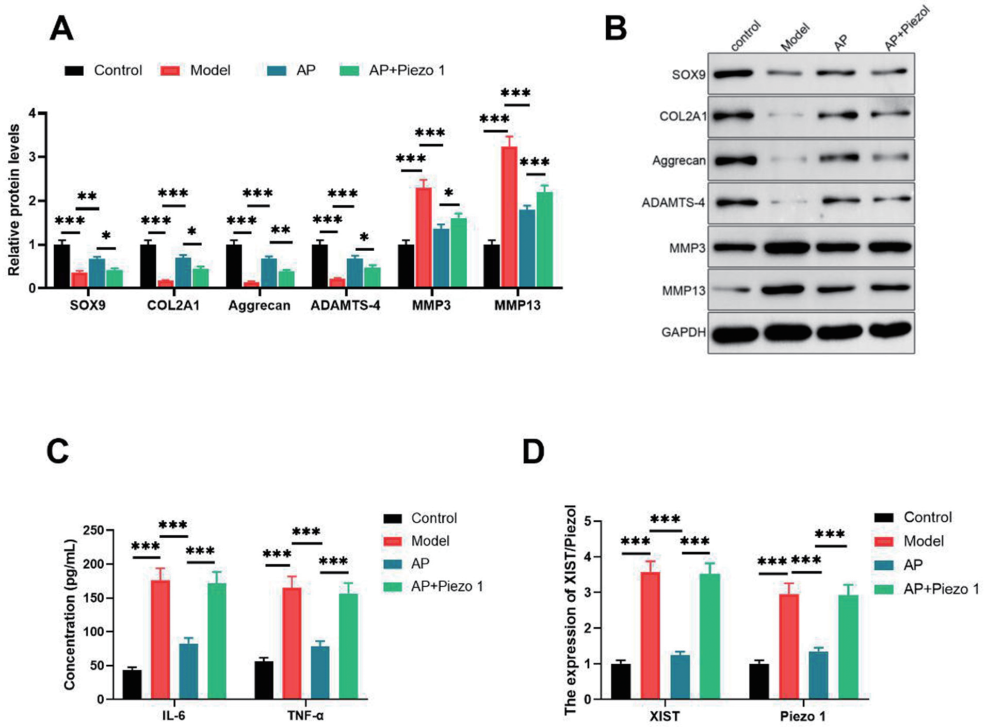


**Fig. 6** Activation of Piezo1 reverses effects of AP treatment among MIA-induced rats

After AP stimulation, and AP stimulation + Piezo1, (A–B) western blot assay accustomed to observing the protein levels of MMP13, MMP3, ADAMTS-4, Aggrecan, COL2A1, SOX9. (C) TNF-α and IL-6 levels. (D) The XIST and Piezo1 mRNA levels. *$P < 0.05$, **$P < 0.01$, ***$P < 0.001$.

AP: acupuncture
MIA: monosodium iodoacetate
MMP: matrix metalloproteinase
COL2A1: recombinant collagen type II alpha 1
SOX9: sex determining region Y box protein 9
XIST: X-inactive specific transcript
IL: interleukin
TNF: tumor necrosis factor
mRNA: messenger RNA
GAPDH: glyceraldehyde-3-phosphate dehydrogenase
ADAMTS: a disintegrin and metalloproteinase with thrombospondin

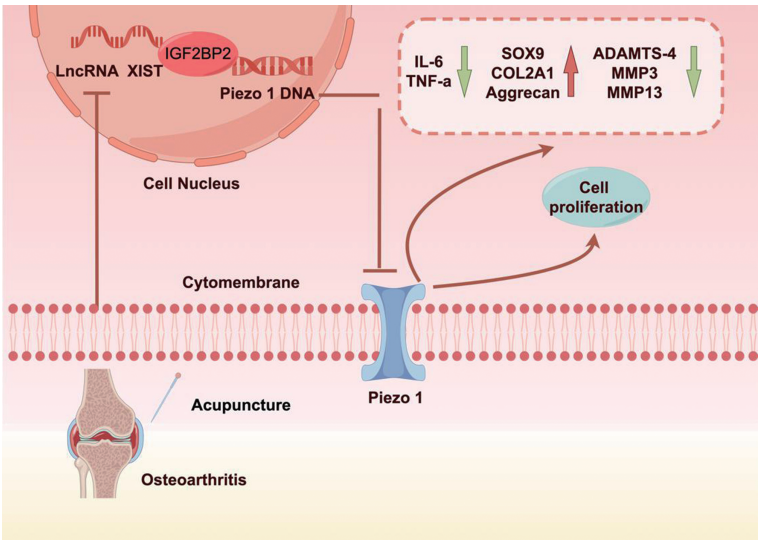


**Fig. 7** Schematic representation illustrating how acupuncture attenuates the progression of knee osteoarthritis by inhibiting XIST-mediated activation of the mechanosensitive ion channel Piezo1 signaling
XIST: X-inactive specific transcript
IGF2BP2: insulin-like growth factor 2 mRNA binding proteins 2
lncRNA: long non-coding RNA
MMP: matrix metalloproteinase
COL2A1: recombinant collagen type II alpha 1
SOX9: sex determining region Y box protein 9
IL: interleukin
TNF: tumor necrosis factor
ADAMTS: a disintegrin and metalloproteinase with thrombospondin

Subsequently, we used ELISA to evaluate changes in the levels of inflammatory factors in each group of animals. The outcomes demonstrated that after AP treatment, the levels of inflammatory factors IL-6 and TNF-α decreased considerably in contrast to the MG (Fig. 6C). However, after Piezo1 agonist treatment, the effect of AP treatment was reversed. Furthermore, PCR accustomed to identifying the expression changes of XIST/Piezo1 in cartilage tissue (Fig. 6D). The results showed that in rats treated with AP, compared to OA model rats, the mRNA levels of XIST and Piezo1 decreased considerably. Then, after Piezo1 agonist treatment, the effect of AP was reversed, and the mRNA levels of XIST and Piezo1 increased significantly, with no difference in contrast to the OA MG. Our research findings indicate that XIST and Piezo1 play a promoting role in OA, promoting the increase of cytokine levels and ECM degeneration.

## DISCUSSION

Modern medicine considers KOA as a degenerative disease, mostly seen in middle-aged and elderly patients.[4] Factors such as aging, trauma, and deformities can exacerbate inflammatory responses. Its pathological features include cartilage erosion, osteophyte formation, degeneration and thickening of the joint capsule, inflammatory synovial fluid production in the joint cavity, and muscle spasms.[20] AP therapy for KOA comes in various forms. AP can promote local circulation of qi and blood, tonify deficiencies and dispel excesses, and achieve effects such as promoting

nourishing the liver and kidneys, alleviating pain, promoting meridian circulation, removing blood stasis and blood circulation. It can also lower levels of inflammatory factors, thereby improving symptoms and slowing the progression of KOA. Many previous clinical studies[18,21] have shown relief in OA patients through AP treatment, but the molecular mechanisms of this treatment are still unclear.

XIST is an RNA gene located on the X chromosome of placental mammals, playing a predominant role in X chromosome inactivation by specifically binding to specific sites on the X chromosome and mediating X chromosome inactivation.[22] Currently, there is extensive research on XIST in cancer, where it regulates disease processes such as cancer cell metastasis, invasion and proliferation.[23] In the recent study related to OA,[24] gene expression profiling chips were searched in Gene Expression Omnibus (GEO) database, and differential gene analysis was performed using R language. It was found that among key long non-coding RNAs in OA patients compared to normal joint tissues, XIST was one of them, showing high expression.[25] Previous studies have shown that compared to CG, serum XIST expression is elevated in OA patients, indicating that high expression of XIST in the serum of KOA patients may affect disease onset.[26] The significance of the research findings lies in uncovering the role of XIST in OA pathogenesis. Our dual siRNA validation approach, showing comparable knockdown efficiency (82.3 ± 4.2% vs 79.8 ± 3.9%) and similar effects on downstream targets including Piezo1, strengthens the specificity of our findings regarding XIST's role in OA pathogenesis. This rigorous validation eliminates concerns about off-target effects and confirms that the observed phenotypes are specifically attributed to XIST knockdown. The study demonstrates that knocking down XIST mRNA significantly enhances the proliferation of CHON-001 cells and reduces apoptosis, suggesting that XIST acts as a promoter of OA process. These findings provide significant perspectives on the molecular mechanisms underlying OA development and emphasize XIST as a possible therapeutic target. Comparing these results with existing research, previous studies have already implicated XIST in various diseases,[27] particularly cancer, where it regulates cellular processes similar to those observed in OA, such as proliferation and apoptosis. The identification of XIST's involvement in OA adds to this body of knowledge and underscores the broader impact of XIST across different disease contexts.

Piezo1 protein has reportedly been implicated in various cellular responses induced by mechanical stress. The research results emphasize the significance of the interaction between lncRNA XIST, Piezo1, and IGF2BP2, particularly in the context of regulating Piezo1 expression. The findings demonstrate that si-XIST significantly decreased Piezo1 expression, indicating a regulatory role of lncRNA XIST in Piezo1 expression. Additionally, IGF2BP2 overexpression reversed the effect of si-XIST, highlighting the participation of IGF2BP2 in mediating the regulatory mechanism of lncRNA XIST on Piezo1 expression. Furthermore, the RIP assay revealed a direct interaction between lncRNA XIST and Piezo1 protein, further substantiating their functional relationship. Overall, these findings shed light on the underlying molecular mechanisms governing Piezo1 expression, offering valuable insights into the regulatory network involving lncRNA XIST and IGF2BP2. Existing studies on Piezo1 expression regulation have highlighted its intricate involvement in various physiological and pathological processes.[28,29] Furthermore, these studies have elucidated the role of Piezo1 in mechano-transduction, immune cell activity, cell volume regulation, migration, and apoptosis.[30,31] Moreover, the molecular mechanisms underlying Piezo1 regulation by lncRNA XIST and IGF2BP2 present a novel perspective on the intricate regulatory pathways governing Piezo1 expression. In KOA, both lncRNA XIST and IGF2BP2 play pivotal roles in the pathogenesis of the condition. The inclusion of an IL-1β+si-NC+Piezo1 overexpression CG in our study confirmed that Piezo1 activation promotes OA progression independently of XIST expression levels, further validating the specificity of the XIST-Piezo1

regulatory axis in OA. This critical control experiment demonstrates that while XIST can regulate Piezo1 expression, Piezo1 activation can override the protective effects of XIST knockdown, indicating that Piezo1 acts downstream of XIST in the pathogenic cascade. LncRNA XIST has been shown to participate in chondrogenic differentiation and the adipogenic and osteogenic differentiation of mesenchymal stem cells, contributing to the progression of OA.[32,33] In OA tissues, an early study demonstrates that lncRNA XIST promotes OA chondrocyte apoptosis and proliferation through the miR-211/CXCR4 axis.[34] Therefore, lncRNA XIST could be a fruitful treatment target to address OA. On the other hand, IGF2BP2's involvement in KOA is through the IGF2BP2/SIRT1 axis and regulation of differentiation antagonizing non-protein coding RNA (DANCR) by affecting N6-methyladenosine (m6A) methylation modification.[35] While the specific evidence of a direct interaction between lncRNA XIST and IGF2BP2 in the context of KOA is not conclusive, the roles of these factors underscore the potential significance of targeting this regulatory axis therapeutically. It presents an opportunity to influence the disease progression by modulating the pathways associated with lncRNA XIST and IGF2BP2. This underscores the need for more study to elucidate the crosstalk between these elements in the context of KOA, thus giving a comprehensive understanding of their relationship and implications. Therefore, a more comprehensive investigation is vital to establish the distinct roles and implications of this regulatory axis in the context of KOA. Specifically, the involvement of lncRNA XIST in modulating Piezo1 expression through the IGF2BP2 pathway adds to our understanding of the complex regulatory networks underlying cellular responses to AP treatment of KOA in this study.

Piezo1 protein generates a large influx of calcium ions under mechanical stress stimulation.[36] Additionally, it has been reported that intracellular calcium overload can trigger oxidative stress damage, depletion of glutathione, and ultimately lead to cell death. These damaging factors can cause changes in chondrocyte number and metabolism, promoting the development of osteoarthritis.[37] In recent studies, it has been found that with high mechanical stress stimulation, activation of Piezo1 protein leads to an increase in intracellular calcium ions.[38,39] Using GSMTx4 to inhibit Piezo1 lessens the calcium ion influx. Furthermore, the role of calcium ions in mediating chondrocyte ferroptosis induced by mechanical stress-activated Piezo1 protein indicates a close relationship between the calcium influx mediated by Piezo1 activation and mechanical stress-induced chondrocyte ferroptosis.[40] Our study indicates that XIST and Piezo1 play a promoting role in OA, promoting the increase of cytokine levels and ECM degeneration. Drawing on our study and prior research, we propose a model elucidating how AP mitigates KOA progression by suppressing XIST-mediated activation of the mechanosensitive ion channel Piezo1 signaling pathway. Upon AP treatment, the Piezo1 channel is inhibited via lncRNA XIST reduction (Fig. 7).

However, there are limitations to consider in our study. Future research directions could focus on elucidating the precise molecular mechanisms of lncRNA XIST-mediated regulation of Piezo1 through the IGF2BP2 pathway. This could involve detailed mechanistic studies using biochemical and molecular approaches to understand the interactions between XIST, IGF2BP2, and Piezo1. Furthermore, exploring the role of this regulatory axis in disease contexts, such as osteoarthritis or other mechanosensitive disorders, could provide insights into potential therapeutic targets or biomarkers. Additionally, investigating the broader impact of lncRNA XIST on cellular physiology and disease progression beyond Piezo1 regulation could uncover novel aspects of its functional role.

## CONCLUSION

In conclusion, our research highlights the therapeutic potential of AP in reducing the progres-

sion of KOA by targeting the XIST-mediated activation of the mechanosensitive ion channel Piezo1 signaling pathway. By inhibiting this pathway, AP may provide a viable strategy for ameliorating the symptoms and slow the progression of KOA. Our comprehensive validation approach, including multiple siRNAs and essential CGs, robustly establishes the specificity of the XIST-Piezo1 pathway in OA progression and AP's therapeutic effect. These rigorous controls strengthen the conclusion that AP specifically targets this pathway to achieve its beneficial effects. Further investigation into the precise mechanisms underlying this therapeutic effect could pave the way for novel interventions in the management of KOA.

## AUTHOR CONTRIBUTIONS

The simulation experiment data used to support the findings of this study are available from the corresponding author upon request.

Guarantor of integrity of the entire study: Huangan Wu, Bimeng Zhang.
Study concepts: Miaomiao Liu.
Study design: Zhaoqin Wang.
Definition of intellectual content: Tao Wu.
Literature research: Yan Ji, Jie Meng.
Clinical studies: Haixin Gou.
Experimental studies: Maoqing Ye, Changfeng Song.
Data acquisition: Miaomiao Liu.
Data analysis: Xingang Lu.
Statistical analysis: Jimeng Zhao.
Manuscript preparation: Tao Wu.
Manuscript editing: Miaomiao Liu.
Manuscript review: Zhaoqin Wang.

## CONFLICTS OF INTEREST

The authors declare that there are no conflicts of interest regarding the publication of this paper.

## FUNDING

None.

## REFERENCES

1 Ma J, Chen X, Xin J, Niu X, Liu Z, Zhao Q. Overall treatment effects of aquatic physical therapy in knee osteoarthritis: a systematic review and meta-analysis. *J Orthop Surg Res*. 2022;17(1):190. doi:10.1186/s13018-022-03069-6

2 Driban JB, Harkey MS, Barbe MF, et al. Risk factors and the natural history of accelerated knee osteoarthritis: a narrative review. *BMC Musculoskelet Disord*. 2020;21(1):332. doi:10.1186/s12891-020-03367-2

3 Primorac D, Molnar V, Rod E, et al. Knee Osteoarthritis: A Review of Pathogenesis and State-Of-The-Art Non-Operative Therapeutic Considerations. *Genes (Basel)*. 2020;11(8):854. doi:10.3390/genes11080854

4 Katz JN, Arant KR, Loeser RF. Diagnosis and Treatment of Hip and Knee Osteoarthritis: A Review. *JAMA*. 2021;325(6):568–578. doi:10.1001/jama.2020.22171

5 Hussain SM, Neilly DW, Baliga S, Patil S, Meek R. Knee osteoarthritis: a review of management options. *Scott Med J*. 2016;61(1):7–16. doi:10.1177/0036933015619588

6 Zhang S, Huang R, Guo G, et al. Efficacy of traditional Chinese exercise for the treatment of pain and disability on knee osteoarthritis patients: a systematic review and meta-analysis of randomized controlled trials. *Front Public Health*. 2023;11:1168167. doi:10.3389/fpubh.2023.1168167

7 Yang M, Jiang L, Wang Q, Chen H, Xu G. Traditional Chinese medicine for knee osteoarthritis: An overview of systematic review. *PLoS One*. 2017;12(12):e0189884. doi:10.1371/journal.pone.0189884

8 Tu JF, Yang JW, Shi GX, et al. Efficacy of Intensive Acupuncture Versus Sham Acupuncture in Knee Osteoarthritis: A Randomized Controlled Trial. *Arthritis Rheumatol*. 2021;73(3):448–458. doi:10.1002/art.41584

9 Coste B, Mathur J, Schmidt M, et al. Piezo1 and Piezo2 are essential components of distinct mechanically activated cation channels. *Science*. 2010;330(6000):55–60. doi:10.1126/science.1193270

10 Wang L, You X, Lotinun S, Zhang L, Wu N, Zou W. Mechanical sensing protein PIEZO1 regulates bone homeostasis via osteoblast-osteoclast crosstalk. *Nat Commun*. 2020;11(1):282. doi:10.1038/s41467-019-14146-6

11 Lai A, Cox CD, Chandra Sekar N, et al. Mechanosensing by Piezo1 and its implications for physiology and various pathologies. *Biol Rev Camb Philos Soc*. 2022;97(2):604–614. doi:10.1111/brv.12814

12 Bella F, Campo S. Long non-coding RNAs and their involvement in bipolar disorders. *Gene*. 2021;796–797:145803. doi:10.1016/j.gene.2021.145803

13 Zhao KP, Wang XY, Shao MQ, He CY, Yuan FQ. Silencing of long noncoding RNA X-inactive specific transcript alleviates Abeta1-42-induced microglia-mediated neurotoxicity by shifting microglial M1/M2 polarization. *Int J Immunopathol Pharmacol*. 2023;37:3946320231184988. doi:10.1177/03946320231184988

14 Liu W, Long Q, Zhang L, et al. Long non-coding RNA X-inactive specific transcript promotes osteosarcoma metastasis via modulating microRNA-758/Rab16. *Ann Transl Med*. 2021;9(10):841. doi:10.21037/atm-21-1032

15 Liu Y, Liu K, Tang C, Shi Z, Jing K, Zheng J. Long non-coding RNA XIST contributes to osteoarthritis progression via miR-149-5p/DNMT3A axis. *Biomed Pharmacother*. 2020;128:110349. doi:10.1016/j.biopha.2020.110349

16 Yang Z, Jiang X, Jiang X, Zhao H. X-inactive-specific transcript: A long noncoding RNA with complex roles in human cancers. *Gene*. 2018;679:28–35. doi:10.1016/j.gene.2018.08.071

17 Ai D, Yu F. LncRNA DNM3OS promotes proliferation and inhibits apoptosis through modulating IGF1 expression by sponging MiR-126 in CHON-001 cells. *Diagn Pathol*. 2019;14(1):106. doi:10.1186/s13000-019-0877-2

18 Wei J, Liu L, Li Z, et al. Fire Needling Acupuncture Suppresses Cartilage Damage by Mediating Macrophage Polarization in Mice with Knee Osteoarthritis. *J Pain Res*. 2022;15:1071–1082. doi:10.2147/JPR.S360555

19 Lee SY, Lee SH, Na HS, et al. The Therapeutic Effect of STAT3 Signaling-Suppressed MSC on Pain and Articular Cartilage Damage in a Rat Model of Monosodium Iodoacetate-Induced Osteoarthritis. *Front Immunol*. 2018;9:2881. doi:10.3389/fimmu.2018.02881

20 Koyama K, Ohba T, Odate T, Wako M, Haro H. Pathological features of established osteoarthritis with hydrathrosis are similar to rheumatoid arthritis. *Clin Rheumatol*. 2021;40(5):2007–2012. doi:10.1007/s10067-020-05453-1

21 Witt C, Brinkhaus B, Jena S, et al. Acupuncture in patients with osteoarthritis of the knee: a randomised trial. *Lancet*. 2005;366(9480):136–143. doi:10.1016/S0140-6736(05)66871-7

22 Borensztein M, Syx L, Ancelin K, et al. Xist-dependent imprinted X inactivation and the early developmental consequences of its failure. *Nat Struct Mol Biol*. 2017;24(3):226–233. doi:10.1038/nsmb.3365

23 Mao H, Wang K, Feng Y, et al. Prognostic role of long non-coding RNA XIST expression in patients with solid tumors: a meta-analysis. *Cancer Cell Int*. 2018;18:34. doi:10.1186/s12935-018-0535-x

24 Zhou Q, Liu J, Xin L, Fang Y, Qi Y, Hu Y. Identification of Characteristic lncRNA Molecular Markers in Osteoarthritis by Integrating GEO Database and Machine Learning Strategies and Experimental Validation. Article in Chinese. *Sichuan Da Xue Xue Bao Yi Xue Ban*. 2023;54(5):899–907. doi:10.12182/20230960101

25 LV G, LI Jun. Correlation analysis of serum lncRNA XIST with the severity and inflammatory factor levels in elderly patients with knee osteoarthritis. *Hebei Med J*. 2023;45(5):671–674.

26 Wang T, Liu Y, Wang Y, Huang X, Zhao W, Zhao Z. Long non-coding RNA XIST promotes extracellular matrix degradation by functioning as a competing endogenous RNA of miR-1277-5p in osteoarthritis. *Int J Mol Med*. 2019;44(2):630–642. doi:10.3892/ijmm.2019.4240

27 Li J, Ming Z, Yang L, Wang T, Liu G, Ma Q. Long noncoding RNA XIST: Mechanisms for X chromosome inactivation, roles in sex-biased diseases, and therapeutic opportunities. *Genes Dis*. 2022;9(6):1478–1492. doi:10.1016/j.gendis.2022.04.007
28 Hong R, Yang D, Jing Y, Chen S, Tian H, Yang Y. PIEZO1-Related Physiological and Pathological Processes in CNS: Focus on the Gliomas. *Cancers (Basel)*. 2023;15(3):883. doi:10.3390/cancers15030883
29 Dienes B, Bazsó T, Szabó L, Csernoch L. The Role of the Piezo1 Mechanosensitive Channel in the Musculoskeletal System. *Int J Mol Sci*. 2023;24(7):6513. doi:10.3390/ijms24076513
30 Cheng Q, Wang L. LncRNA XIST serves as a ceRNA to regulate the expression of ASF1A, BRWD1M, and PFKFB2 in kidney transplant acute kidney injury via sponging hsa-miR-212-3p and hsa-miR-122-5p. *Cell Cycle*. 2020;19(3):290–299. doi:10.1080/15384101.2019.1707454
31 Arenas GA, Valenzuela JG, Peñaloza E, et al. Transcriptional Profiling of Human Endothelial Cells Unveils PIEZO1 and Mechanosensitive Gene Regulation by Prooxidant and Inflammatory Inputs. *Antioxidants (Basel)*. 2023;12(10):1874. doi:10.3390/antiox12101874
32 Jankowski M, Farzaneh M, Ghaedrahmati F, et al. Unveiling Mesenchymal Stem Cells' Regenerative Potential in Clinical Applications: Insights in miRNA and lncRNA Implications. *Cells*. 2023;12(21):2559. doi:10.3390/cells12212559
33 Zhu Y, Li R, Wen LM. Long non-coding RNA XIST regulates chondrogenic differentiation of synovium-derived mesenchymal stem cells from temporomandibular joint via miR-27b-3p/ADAMTS-5 axis. *Cytokine*. 2021;137:155352. doi:10.1016/j.cyto.2020.155352
34 Li L, Lv G, Wang B, Kuang L. The role of lncRNA XIST/miR-211 axis in modulating the proliferation and apoptosis of osteoarthritis chondrocytes through CXCR4 and MAPK signaling. *Biochem Biophys Res Commun*. 2018;503(4):2555–2562. doi:10.1016/j.bbrc.2018.07.015
35 Nan Y, Chen M, Wu W, et al. IGF2BP2 regulates the inflammation of fibroblast-like synoviocytes via GSTM5 in rheumatoid arthritis2023. *Cell Death Discov*. 2024;10(1):215. doi:10.1038/s41420-024-01988-3
36 Wong TY, Juang WC, Tsai CT, et al. Mechanical Stretching Simulates Cardiac Physiology and Pathology through Mechanosensor Piezo1. *J Clin Med*. 2018;7(11):410. doi:10.3390/jcm7110410
37 Zahan OM, Serban O, Gherman C, Fodor D. The evaluation of oxidative stress in osteoarthritis. *Med Pharm Rep*. 2020;93(1):12–22. doi:10.15386/mpr-1422
38 Syeda R, Xu J, Dubin AE, et al. Chemical activation of the mechanotransduction channel Piezo1. *Elife*. 2015;4:e07369. doi:10.7554/eLife.07369
39 Romac JM, Shahid RA, Swain SM, Vigna SR, Liddle RA. Piezo1 is a mechanically activated ion channel and mediates pressure induced pancreatitis. *Nat Commun*. 2018;9(1):1715. doi:10.1038/s41467-018-04194-9
40 Wang S, Li W, Zhang P, et al. Mechanical overloading induces GPX4-regulated chondrocyte ferroptosis in osteoarthritis via Piezo1 channel facilitated calcium influx. *J Adv Res*. 2022;41:63–75. doi:10.1016/j.jare.2022.01.004